

NANO EXPRESS

Open Access



# Flexible Field Emitter for X-ray Generation by Implanting CNTs into Nickel Foil

Bin Sun, Yan Wang and Guifu Ding\*

## Abstract

This paper reports on a flexible Ni micro wire with CNTs embedded into its surface. By using micromachining technology, for the first time, we could implant nanoscale materials into micro-scale metal substrate at room temperature. Thanks to the effective direct contact and the strong interactions between CNTs and the substrate, field emission current of 1.11 mA (current density of 22.2 mA/cm<sup>2</sup>) could be achieved from the micro wire. Moreover, the wire shows excellent mechanical properties for large amplitude bending, which is beneficial for geometric designing. To check the practical application of the wire, a simplified X-ray imaging system was set up by modifying a conventional tube. The gray shade that appears on the sensitive film after being exposed to the radiation confirms the X-ray generation.

**Keywords:** Micromachining, Carbon nanotube, Field emission, X-ray generation

## Background

CNTs have attracted considerable interest for use in field emission devices on account of their extraordinary mechanical, chemical, and electrical properties [1], although high-performance CNT field emitters with emission current over 1 mA have already been achieved [2, 3], flexible CNT emitter with emission current over 1 mA has not been reported. It is believed that CNT field emitters have not reached their full potential and there are still lots of challenges in this field.

Flexible electronic devices have recently attracted great attention for their diverse applications such as bendable sensors [4], flexible displays [5] and X-ray radiotherapy. Most studies have attempted to fabricate CNT emitters on polymeric substrates for flexibility purposes by using electrophoretic method [6], direct growth [7], transfer [8, 9], and wet coating [5]. Those methods have many merits in preparing CNT emitters such as simple processes and controllable loading of CNTs. However, low thermal conductivity and low thermal degeneration temperature of the polymer substrate can lead to joule heating of the interface [10], thereby damaging the

emitter interface and resulting in the increasing of turn-on field over extended periods [11].

Metal substrates, with good mechanical properties and high thermal conductivity, seem to be the most promising substrate for low-cost, flexible, and arbitrary shaped emitters. In general, metal-based CNT emitters were fabricated by screen printing [12] or direct growth [13]. CNTs on those emitters were bonded to the substrates only by van der Waals interaction; the adhesion between the CNTs and the substrate is low [14]. The emitter structure and morphology can be easily damaged under complex curving conditions, which leads to fatal breakdown or arcing during device operation [15].

In this research, we propose a micromachining method to solve these problems. By using this technique, CNTs are firmly embedded into the Ni micro wire. Ni has been widely used as an adhesion wetting layer for the CNT field emitters due to its high adhesive strength and electrical conductivity [16]. Effective direct contact between CNTs and the metal substrate was achieved, which would be crucial for low contact resistance. Meanwhile, as the CNT tips were firmly buried into the substrate, there would hardly be any detachment of CNTs from the substrate induced by weak adhesion. By optimum geometric design, the micro wire shows excellent mechanical properties for planar

\* Correspondence: gfding@sjtu.edu.cn

National Key Laboratory of Micro/Nano Fabrication Technology, School of Electronic Information and Electrical Engineering, Shanghai Jiao Tong University, Shanghai 200240, People's Republic of China

supporting and large amplitude bending. To check the application of the micro wire, an X-ray imaging experiment is performed. A simple diode X-ray tube is achieved by sealing the twisted wire into a conventional X-ray tube. The gray shade obtained from the X-ray system confirms the generation of X-rays using our electron source.

**Methods**

The CNT composite paste composed of multi-walled CNTs (purity more than 95 %, diameter 30–50 nm, length 5–15 μm) and polyimide (PI, absolute viscosity 1100–1200 mPa s). To maintain the intrinsic properties of CNTs, no surfactant was added to the paste. And the homogeneous CNT-PI paste was achieved using just ball-milling apparatus. In this research, PI is used as sacrificial medium. The preparation process is presented as follows (Fig. 1):

- (1) The homogeneous CNT-PI paste was spun on the glass wafer, CNT/PI film was formed by baking at 90 °C for 2 h, and then the film was polished.
- (2) Selective chemical etching was carried out, a thin layer of PI of micron level was etched away from the PI/CNT film, and a flat surface with protruding tips of CNTs was achieved.
- (3) Ni wetting layer was sputtered on the above flat surface and covered the protruding tips of CNTs.

- (4) Photoresist of 50 μm was spun on the Ni layer, and lithography was performed to develop the pattern area for Ni substrate.
- (5) Then Ni film of 50 μm (the reasons for choosing Ni as the basement were its resistance to corrosion, and favorable mechanical properties) was fabricated by electroplating on the Ni conducting layer.
- (6) Selective chemical etching was carried out to remove the remaining PI and photoresist. The wafer was immersed in the etchant (composed of sodium hydroxide, ethyl alcohol, and sodium hydrogen phosphate), and sonicated for 30 min and flushed by deionized water. A contaminant-free method, rolling by a soft-rubber roller was used for post treatment, and then the Ni film emitter (the image was rotated 180°) with free standing CNTs on its surface was achieved.

All the above steps were carried out at room temperature. And the inset images were CNT morphology before and after the sputtering process.

**Results and Discussion**

Figure 2a shows the optical images of the fabricated micro wire (100 × 50 × 50,000 μm<sup>3</sup>). By choosing Ni as the substrate material, the wire showed good mechanical properties for planar supporting and large amplitude bending, it could even be twisted and rolled up. The

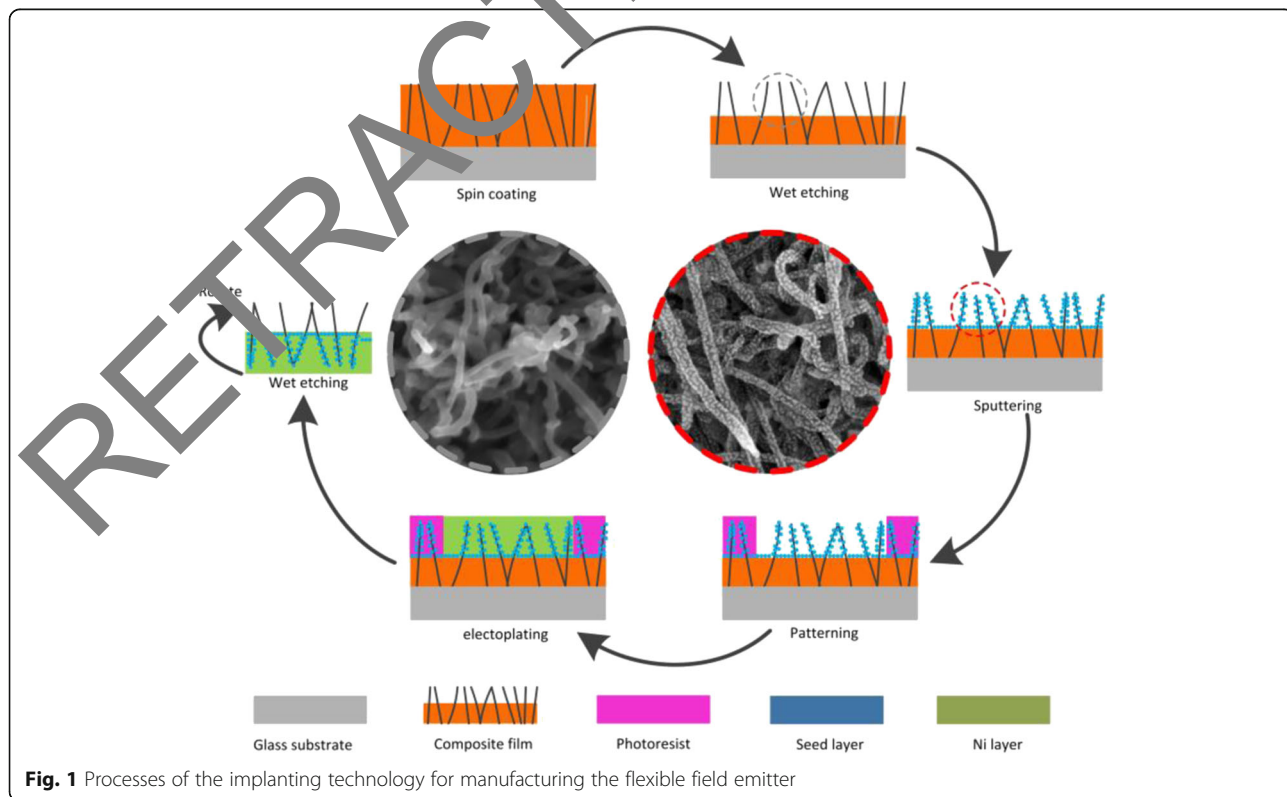


**Fig. 1** Processes of the implanting technology for manufacturing the flexible field emitter

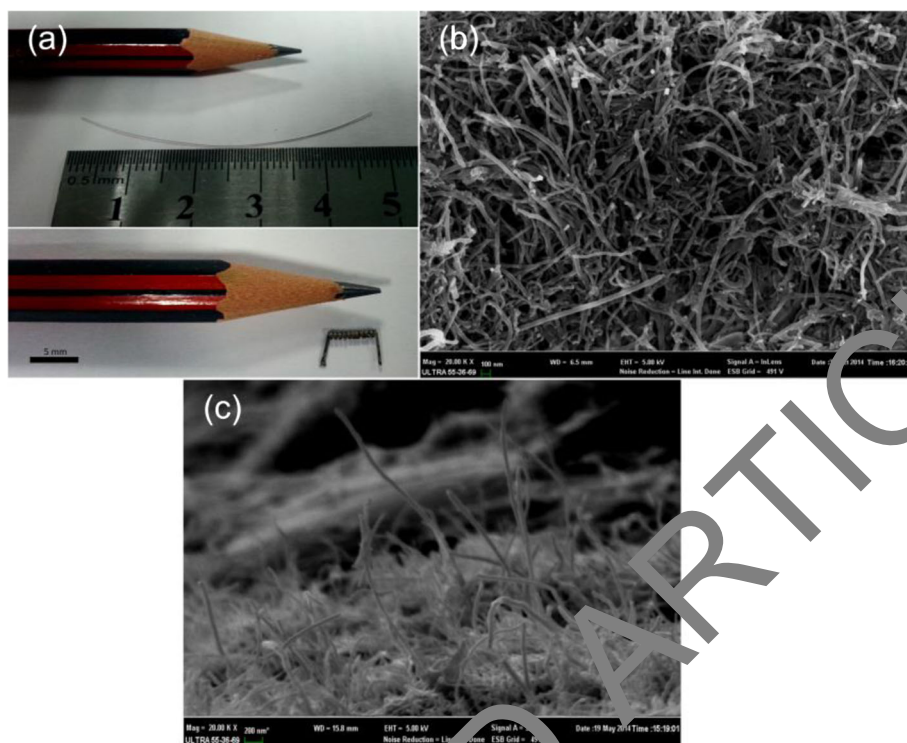


**Fig. 2** a Optical images of the fabricated micro wire (straight and twisted), (b, c) SEM images of the wire surface covered by CNTs

wire surface morphology was inspected by SEM. From the images (Fig. 2b, c), we can see that the micro wire is totally covered by randomly oriented CNTs. The density of CNTs exposed on the micro wire after fabrication steps is around  $33 \text{ tips}/\mu\text{m}^2$ . The CNT tips were firmly embedded in the substrate and no contamination was induced. In addition, CNT distribution was well controlled by the micromachining process. The vertical alignment of the CNTs on the surface actively contributed to stable electron emission when an electric field was applied.

The structural changes that induced by the ball milling process were inspected by TEM. From the TEM images, we can see that the ball-milling treatment decreases the length of the CNT. For the untreated nanotubes (Fig. 3a, b) only some tips can be seen and most of them belong to different nanotubes. In fact, the tubes are too long to fit in a single TEM image. After the ball milling process, some of the broken nanotubes can be measured (those shorter than  $10 \mu\text{m}$ ). Typical nanotubes with open tips can be seen in Fig. 3c, d. And disordered carbon which proved to be multi-layered polyaromatic carbon could also be observed [17].

As shown in Fig. 4, the two sharp peaks at approximate  $1350 \text{ cm}^{-1}$  (D band) and  $1580 \text{ cm}^{-1}$  (G band) representing typical characteristics of amorphous and graphite carbons, respectively. The appearance of those

two peaks in the emitter surface indicated that the CNTs were successfully transferred onto the Ni substrate by the micromachining technology. The D band at approximate  $1350 \text{ cm}^{-1}$  is generally attributed to defects in the curved graphite sheet or other impurities, while the G band at approximate  $1580 \text{ cm}^{-1}$  is corresponding to the opposite direction movement of two neighboring carbon atoms in a graphitic sheet, and it indicates the presence of crystalline graphitic carbon in CNTs [18]. From the results, we can see that the  $I_D/I_G$  ratio of the pristine CNT is 0.70, it increases to 0.99 after the ball-milling process, indicating decreased crystallinity that was attributed to both cutting and destruction of carbon nanotubes [17, 19]. The main reason for this phenomenon is that the ball milling process was used to disperse CNTs into the transfer media (PI). Due to their small tip radius and high aspect ratio, CNTs have highly entangled structure, which needs to be dispersed, preferably up to single nanotube level, for practical applications. During the ball milling process, large CNT aggregate (composed of many CNTs) broke up, and CNTs turned into conglomeration which was closed to granules and sheets because of the friction of rolling between the balls. It is to say that the ball milling process not only decreased the CNT aggregate size but also induced CNT disruption and the production of disordered carbon. The  $I_D/I_G$  ratio decreases from 0.99 to 0.85 after the fabrication process.

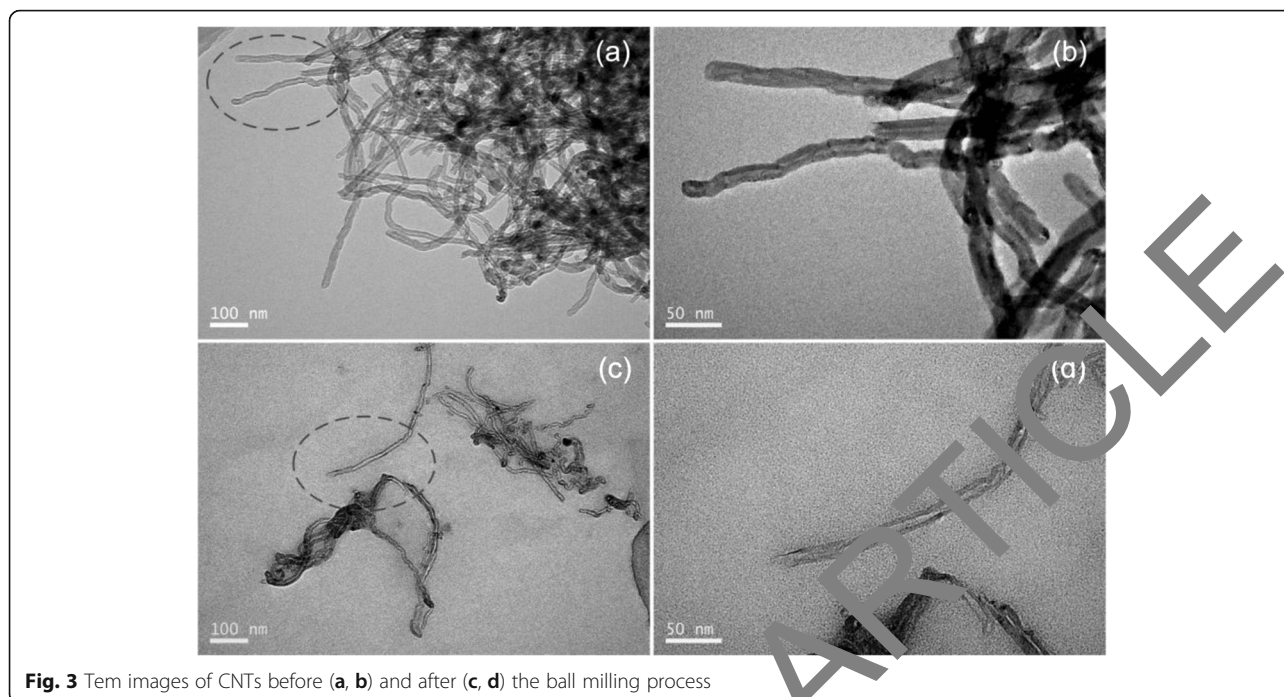


**Fig. 3** Tem images of CNTs before (a, b) and after (c, d) the ball milling process

It is speculated that there are two main reasons for this phenomenon. Firstly, the CNTs with defects attributed to destruction of carbon nanotubes showing relatively poor mechanical properties were more easily cut off into short pieces during the ball milling process. Then, short CNTs were more easily dropped out compared with longer CNTs during the selective wet etching process (process 2). In other words, CNTs with less disordered carbon were more easily to survive during the fabrication process and be transferred in to the micro wire, which resulted in the improvement of crystallinity comparing with the milled CNTs in the Raman spectra.

The field emission characteristics of the samples were measured in a vacuum chamber with a parallel diode-type configuration at pressure of  $1 \times 10^{-6}$  Tor. A mica sheet of 200  $\mu\text{m}$  was used as spacer. In order to protect high-voltage power supply from high-voltage arcing breakdown, a current-limiting resistor (5 M $\Omega$ ) was used. An aging process was carried out with an applied voltage of 800 V for 12 h before the test. During the aging process, arcing occurred occasionally. Since CNTs of greater heights contribute to higher field emission current, thermal runaway is more serious at longer CNTs. As a result, longer CNTs became short and

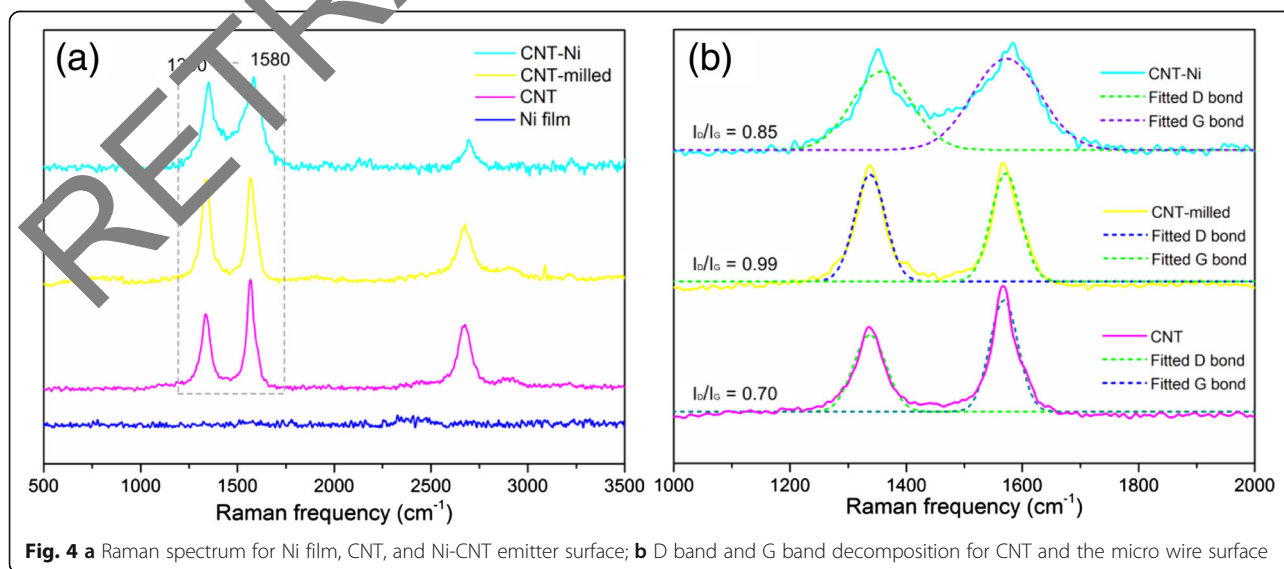


**Fig. 4** a Raman spectrum for Ni film, CNT, and Ni-CNT emitter surface; b D band and G band decomposition for CNT and the micro wire surface

vertically standing CNTs with more uniform heights remained on the Ni substrate after the aging process. The emission current vs. applied electric voltage were repeatedly measured (in Fig. 5), the  $I$ - $V$  curves remained almost constant at the repeated field emission tests. The emission current increases monotonically with the applied field. The turn-on field that defined as an electric field required getting an emission current of  $10\ \mu\text{A}$  was  $1.56\ \text{V}/\mu\text{m}$ . We simply consider the area of the micro wire as the field emission area. The area  $S = 0.01 \times 5 = 0.05\ \text{cm}^2$ . With the applied field of  $3.65\ \text{V}/\mu\text{m}$ , the field emission current of  $1.11\ \text{mA}$  and the current density of  $22.2\ \text{mA}/\text{cm}^2$  was achieved. In Fig. 5, the emission current curve seems to show a “linear” relation with the applied field from  $550$  to  $650\ \text{V}$ . This phenomenon was caused by the current-limiting resistor who shared the voltage of the field emitter in the circuit. The corresponding Fowler-Nordheim (F-N) plot for the flexible emitter is shown in the inset of Fig. 5. All dots on the curve fit a single straight line well, which implies that the field emission process follows the F-N mechanism.

Before continuous emission measurement, an aging process was carried out for  $12\ \text{h}$  with driving condition of a higher applied voltage at  $800\ \text{V}$ . And the short-term stability of CNT field emitter was evaluated by monitoring emission current under constant DC operation for  $60\ \text{h}$ . As shown in Fig. 6, with applied field of  $2.16$ ,  $2.4$ ,  $2.74$ , and  $3.07\ \text{V}/\mu\text{m}$ , emission current of  $53.1$ ,  $103.6$ ,  $203.6$ , and  $400.3\ \mu\text{A}$  could be achieved, and they remained almost constant during the  $60\ \text{h}$  continuous measurement, and the fluctuation width of the emission current for  $60\ \text{h}$  were all in  $\pm 5\%$ . One thing to note here is that a few arcing events occurred when the emission current reached higher than  $400\ \mu\text{A}$ . However, the emitter could withstand the arcing and the emission current remained constant with time. The stable emission

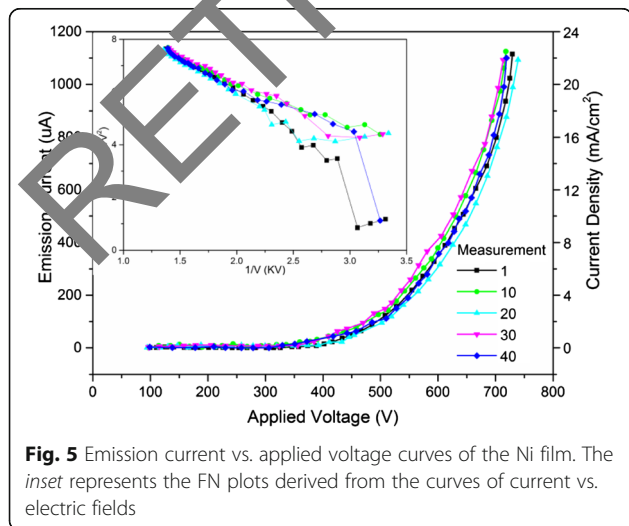


**Fig. 5** Emission current vs. applied voltage curves of the Ni film. The inset represents the FN plots derived from the curves of current vs. electric fields

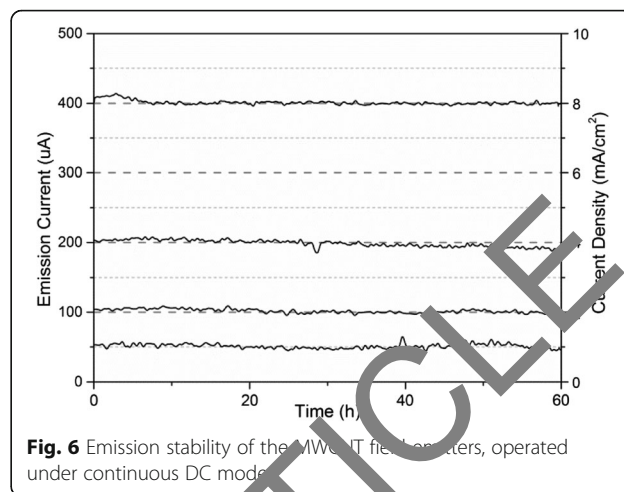


**Fig. 6** Emission stability of the Ni/CNT field emitters, operated under continuous DC mode

performance was primarily due to the firm, direct bonding between CNT and Ni substrate, which greatly reduces the contact resistance between CNTs and substrate and the damage of CNTs escaping from the emitter surface (Arcing accompanied with high current flow can be initiated by the CNTs detachment, and the cathode can be seriously damaged [15]).

In this section, the experiments are presented that prove the X-ray generation with the electron source described in the previous sections. The fabricated emitter was sealed in a conventional X-ray tube, as shown in Fig. 7b,c. The diameter of the glass shell around the anode is  $30\ \text{mm}$ , while the diameter of the glass shell around the cathode is  $20\ \text{mm}$ . All of the connection parts of the X-ray tube were tightly vacuum-sealed. The distance between cathode and anode was maintained at  $10\ \text{mm}$ . The proof of the X-ray creation was done by using an X-ray sensitive film. This film was commercially available (Kodak Insight,  $31 \times 41\ \text{mm}^2$ ) and widely used in dental diagnostics as standard X-ray analogue film plates. The detection was done by placing the film in front of the anode outside the glass shell. The sealed X-ray tube was successfully operated at  $30\ \text{KV}$  with an extraction current from the cathode of  $307\ \mu\text{A}$ . As the emitter was fixed in a “cap,” the electric field between cathode and anode was complex. The X-ray tube can be operated under a relatively low voltage compared with other works [20–22]. A round badge with a thickness of  $100\ \mu\text{m}$  and diameter of  $3\ \text{mm}$  was put in front of the sensitive plate in order to create a defined pattern when exposed to radiation, the shadow of the aperture thus unequivocally confirms the X-ray emission. The sensitive plate and the badge were exposed to the radiation under emission current of  $307\ \mu\text{A}$  for  $30\ \text{min}$  to compensate for the X-ray energy loss. The above exposed plate was then developed in accordance with the photographic processing. The photograph of the badge and the

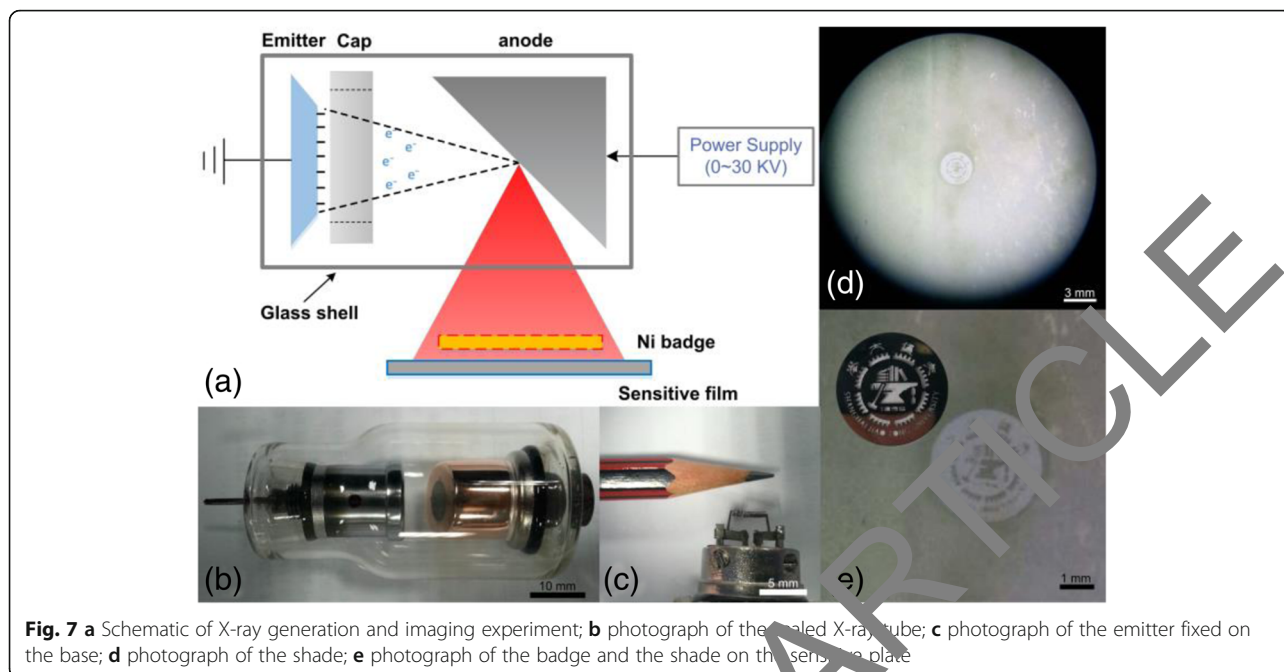


**Fig. 7** **a** Schematic of X-ray generation and imaging experiment; **b** photograph of the sealed X-ray tube; **c** photograph of the emitter fixed on the base; **d** photograph of the shade; **e** photograph of the badge and the shade on the sensitive film

developed copy can be seen in Fig. 6. The blackened shade on this copy confirms the X-ray generation, which demonstrates that our emitter successfully survived the high temperature processing steps of the X-ray source fabrication.

## Conclusions

In summary, we have introduced a flexible Ni micro wire with CNTs embedded into its surface fabricated by micromachining. Direct contact and strong interactions between CNTs and the metal substrate contribute to its high current field emission performance such as low turn on field (1.56 V/ $\mu\text{m}$ ), high emission current (1.11 A, current density  $22 \text{ A/cm}^2$ ), and good stability (60 h for 5 % fluctuation of emission current around 400  $\mu\text{A}$ ). The novel wire showed great potential used for X-ray tube electron source. The gray shade that appears on the sensitive film after being exposed to the radiation confirms the X-ray generation from the vacuum sealed tube. It is believed that this report must be helpful for high current flexible CNT field emitter development, yet further optimization in device configuration and cathode structure is required.

## Abbreviations

CNT: Carbon nanotube; PI: Polyimide

## Acknowledgements

The authors express their sincere gratitude to the colleagues of National Key Laboratory of Nano/Micro Fabrication Technology. The authors would like to appreciate the support from the National Natural Science Foundation of China (No. 51305265, No. 51205390) and the Research Fund for the Doctoral Program of Higher Education of China (No.20120073110061).

## Authors' Contributions

BS carried out the design and fabrication of the experimental setups and drafted the manuscript. GD supervised the whole study. YW participated in the preparation of the carbon nanotube field emitter and assisted in the experiments. All authors read and approved the final manuscript.

## Competing Interests

The authors declare that they have no competing interests.

Received: 8 June 2016 Accepted: 20 August 2016

Published online: 10 September 2016

## References

1. Fan SS, Chapline MG, Franklin NR, Tomblor TW, Cassell AM, Dai HJ (1999) Self-oriented regular arrays of carbon nanotubes and their field emission properties. *Science* 283:512–514
2. Xiomara C-C, Huaizhi G, Bo G, Lei A, Guohua C, Otto Z (2009) A carbon nanotube field emission cathode with high current density and long-term stability. *Nanotechnology* 20:325707
3. Zhu W, Bower C, Zhou O, Kochanski G, Jin S (1999) Large current density from carbon nanotube field emitters. *Appl Phys Lett* 75:873–875
4. Kanoun O, Muller C, Benchirouf A, Sanli A, Dinh TN, Al-Hamry A, Bu L, Gerlach C, Bouhamed A (2014) Flexible carbon nanotube films for high performance strain sensors. *Sensors-Basel* 14:10042–10071
5. Jung H, An SY, Jang DM, Kim JM, Park JY, Kim D (2012) A multi-wall carbon nanotube/polymethyl methacrylate composite for use in field emitters on flexible substrates. *Carbon* 50:987–993
6. Zhang JH, Zang JB, Huang JJ, Wang YH, Xin GX (2014) Synthesis of an architectural electrode based on manganese oxide and carbon nanotubes for flexible supercapacitors. *Mater Lett* 126:24–27
7. Jeong HJ, Jeong HD, Kim HY, Kim JS, Jeong SY, Han JT, Bang DS, Lee G-W (2011) All-carbon nanotube-based flexible field-emission devices: from cathode to anode. *Adv Funct Mater* 21:1526–1532
8. Jung YJ, Kar S, Talapatra S, Soldano C, Viswanathan G, Li XS, Yao ZL, Ou FS, Avadhanula A, Vajtai R, Curran S, Nalamasu O, Ajayan PM (2006) Aligned carbon nanotube-polymer hybrid architectures for diverse flexible electronic applications. *Nano Lett* 6:413–418
9. Shin DH, Jung SI, Yun KN, Chen G, Song Y-H, Saito Y, Milne WI, Lee CJ (2014) Field emission properties from flexible field emitters using carbon nanotube film. *Appl Phys Lett* 105:033110

10. Kumar A, Pushparaj VL, Kar S, Nalamasu O, Ajayan PM, Baskaran R (2006) Contact transfer of aligned carbon nanotube arrays onto conducting substrates. *Appl Phys Lett* 89:163120
11. Kottler C, Longtin R, Giudice S, Jose-James R, Niedermann P, Neels A, Kaufmann R, Sanchez-Valencia JR, Elsener HR, Groning O, Leinenbach C, Groning P, Dommann A (2014) X-ray source downscaling enabled by combining microfabricated electrodes with carbon nanotube cold electron emitters. *Microelectron Eng* 122:13–19
12. Kim J-W, Jeong J-W, Kang J-T, Choi S, Park S, Shin M-S, Ahn S, Song Y-H (2015) Great improvement in adhesion and uniformity of carbon nanotube field emitters through reactive nanometer-scale SiC fillers. *Carbon* 82:245–253
13. Heo SH, Ihsan A, Cho SO (2007) Transmission-type microfocus X-ray tube using carbon nanotube field emitters. *Appl Phys Lett* 90:183109
14. Lee J, Jung Y, Song J, Kim JS, Lee G-W, Jeong HJ, Jeong Y (2012) High-performance field emission from a carbon nanotube carpet. *Carbon* 50: 3889–3896
15. Ha JM, Kim HJ, Raza HS, Cho SO (2013) Highly stable carbon nanotube field emitters on small metal tips against electrical arcing. *Nanoscale Res Lett* 8: 355
16. Lee H, Goak J, Choi J, Kong B, Lee CH, Kim KB, Park J-Y, Seo Y, Choi YC, Song YH, Lee N (2012) High-current field emission of point-type carbon nanotube emitters on Ni-coated metal wires. *Carbon* 50:2126–2133
17. Pierard N, Fonseca A, Colomer JF, Bossuot C, Benoit JM, Van Tendeloo G, Pirard JP, Nagy JB (2004) Ball milling effect on the structure of single-wall carbon nanotubes. *Carbon* 42:1691–1697
18. Wei G (2006) Emission property of carbon nanotube with defects. *Appl Phys Lett* 89:143111
19. Pierard N, Fonseca A, Konya Z, Willems I, Van Tendeloo G, Nagy JB (2001) Production of short carbon nanotubes with open tips by ball milling. *Chem Phys Lett* 335:1–8
20. Heo SH, Kim HJ, Ha JM, Cho SO (2012) A vacuum-sealed miniature X-ray tube based on carbon nanotube field emitters. *Nanoscale Res Lett* 7:258
21. Jeong J-W, Kang J-T, Choi S, Kim J-W, Ahn S, Song Y-H (2013) A digital miniature X-ray tube with a high-density triode carbon nanotube field emitter. *Appl Phys Lett* 102:023504
22. Jin-Woo J, Jae-Woo K, Jun-Tae K, Sungyoul C, Seungjoon A, Yong-Ho H (2013) A vacuum-sealed compact X-ray tube based on focused carbon nanotube field-emission electrons. *Nanotechnology* 24:085201

RETRACTED ARTICLE

Submit your manuscript to a SpringerOpen<sup>®</sup> journal and benefit from:

- Convenient online submission
- Rigorous peer review
- Immediate publication on acceptance
- Open access: articles freely available online
- High visibility within the field
- Retaining the copyright to your article

---

Submit your next manuscript at ► [springeropen.com](http://springeropen.com)

---